Polar Materials and Ferroelectrics

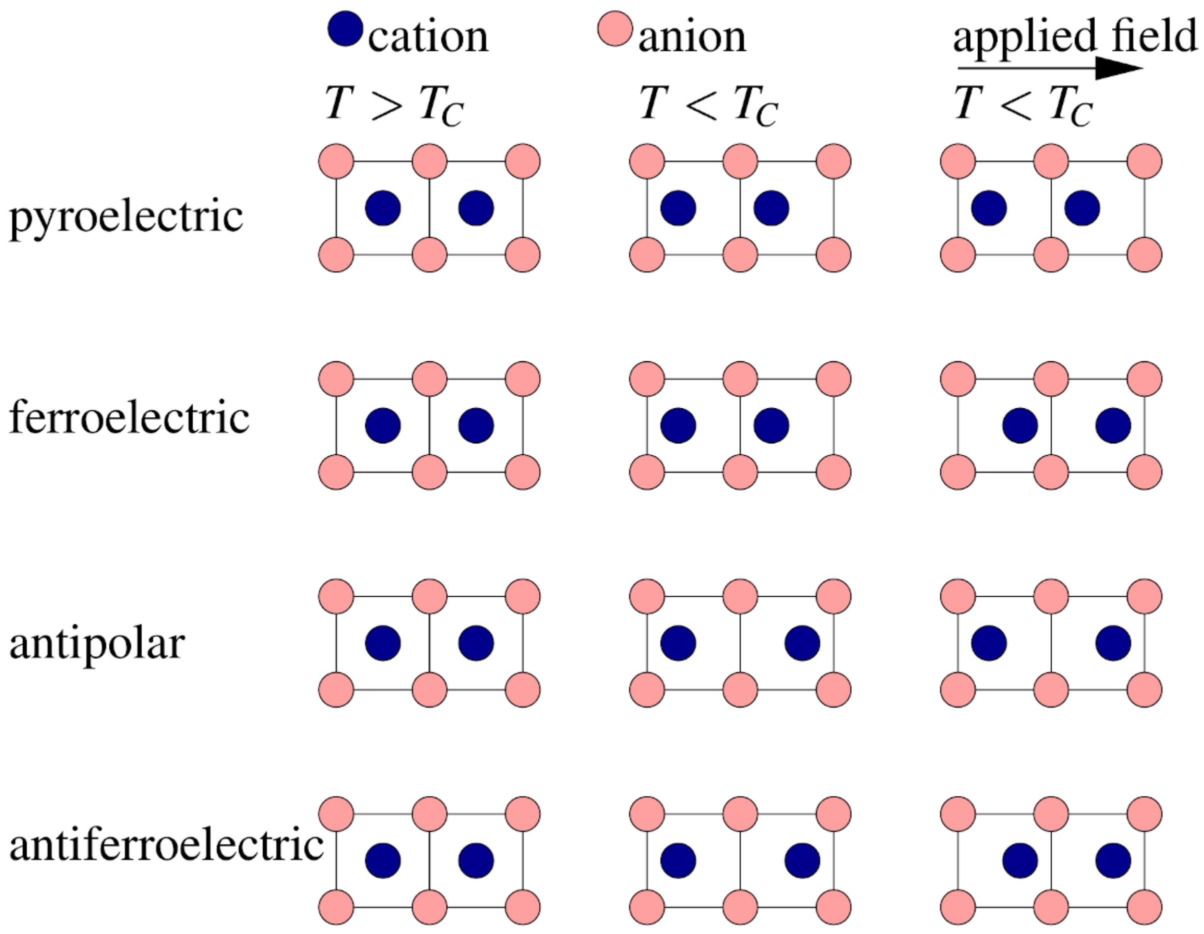

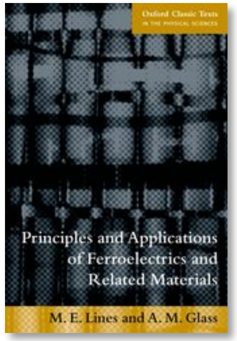

Principles and Applications of Ferroelectrics and Related
M. E. Lines, A. M. Glass. OUP Oxford, 2001

All of these materials display thermal phase transitions to a compound with a polar point group

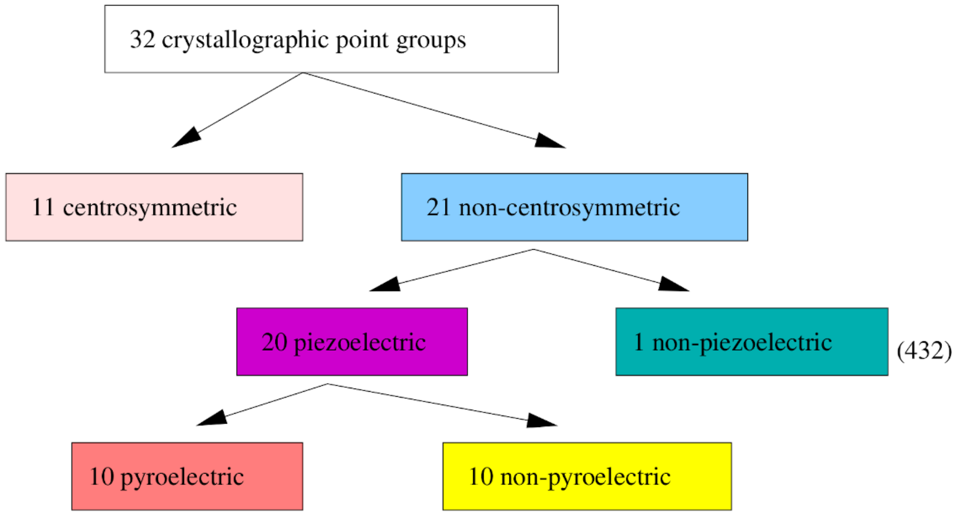

Polar Materials and Ferroelectrics

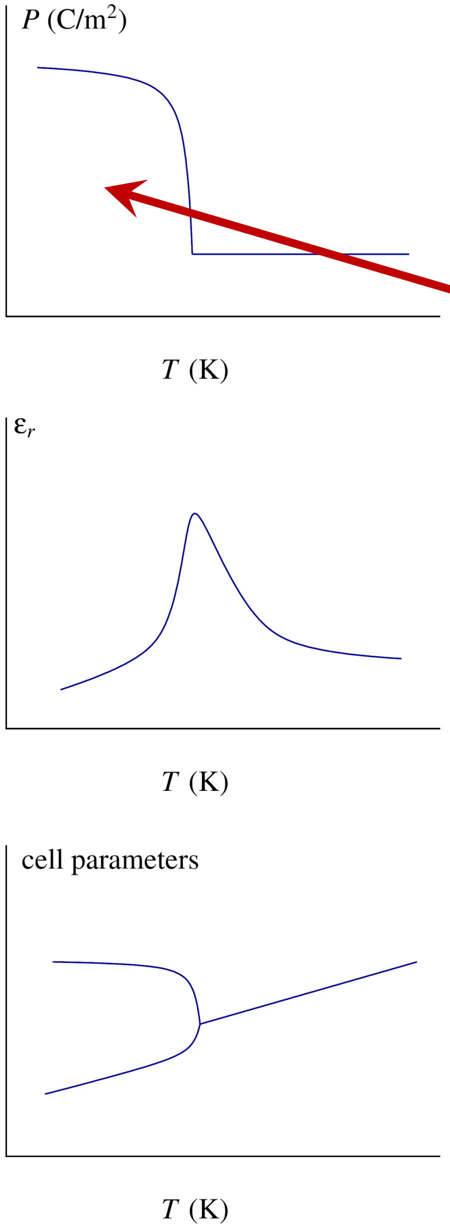

Thermal evolution of a ferroelectric

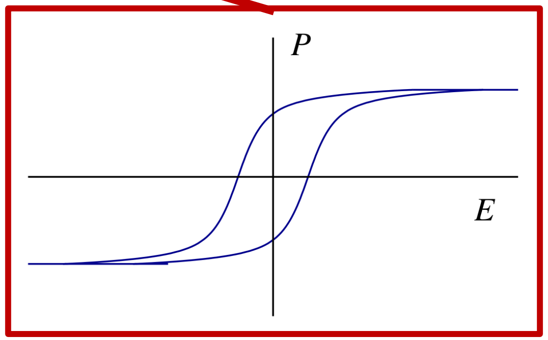

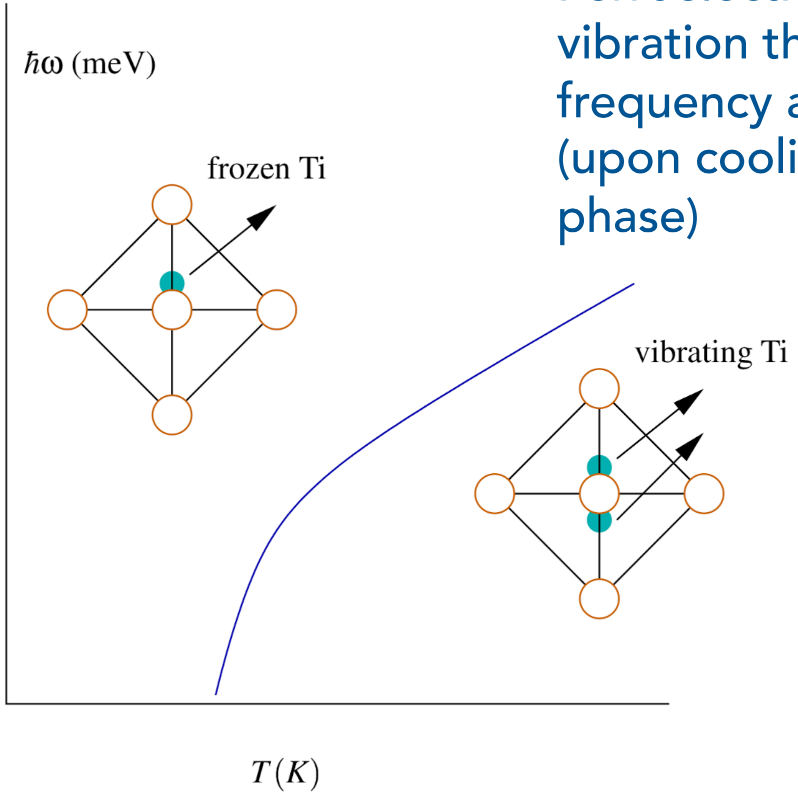

Ferroelectric soft mode: A vibration that goes to 0 frequency at the transition (upon cooling to the polar phase)

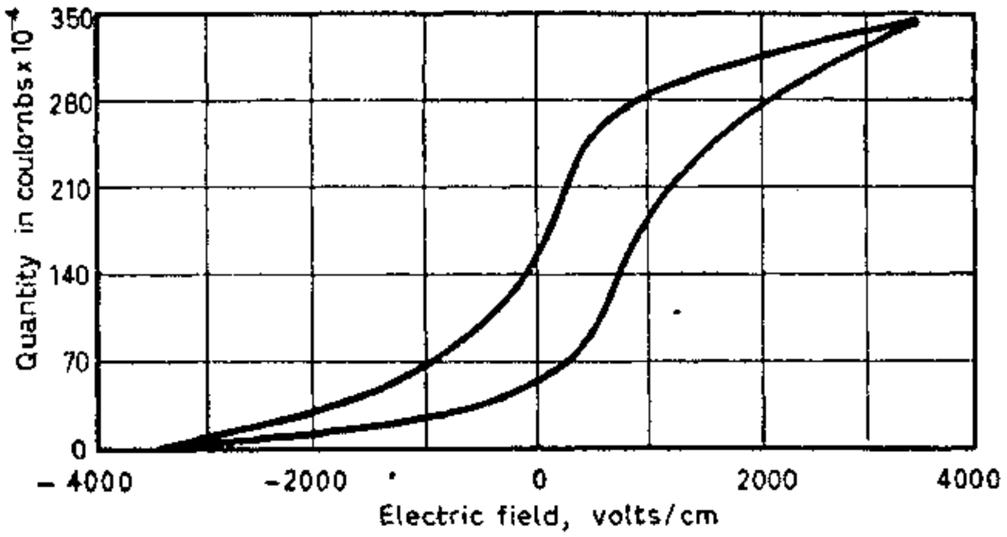

Fig. 1.1. Dielectric hysteresis loop for Rochelle salt (Valasek, 1921).

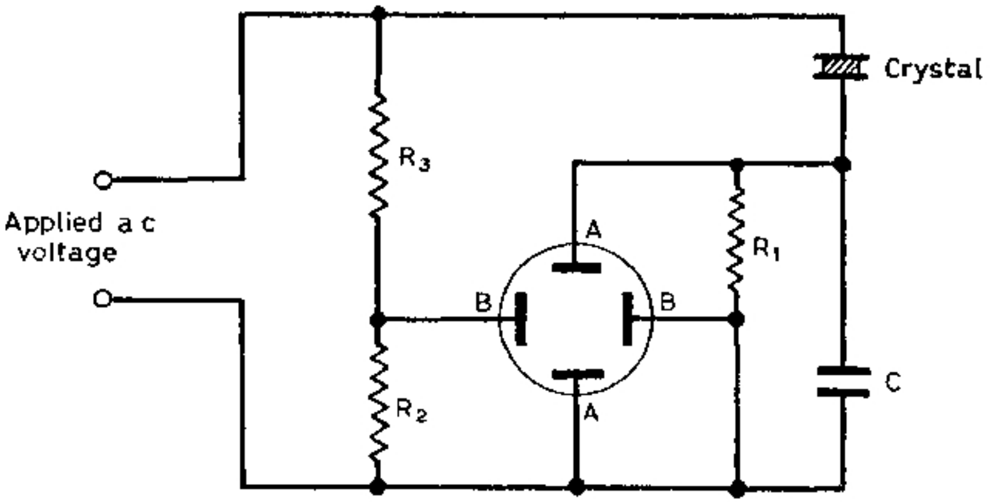

Fig. 1.2. Circuit for investigating hysteresis loop (Sawyer and Tower, 1930).

The original discovery by Valacek in Rochelle salt, in 1921. The Sawyer-Tower circuit for measurements is shown below.

Rochelle salt: Potassium sodium tartrate tetrahydrate, ($KNaC_4H_4O_6 \cdot 4H_2O$)

David Brewster in 1824 demonstrated piezoelectric effects thereon, which led to him naming the effect pyroelectricity.

From H. W. Megaw, Ferroelectricity in Crystals, Methuen, London, 1957

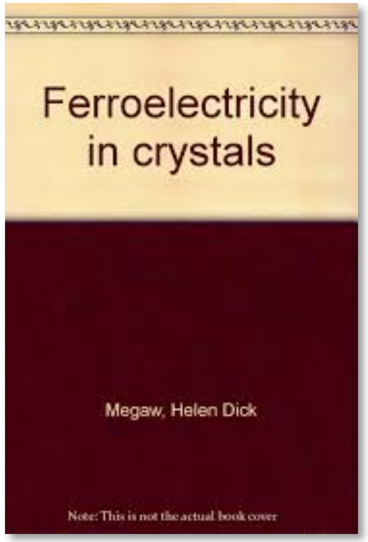

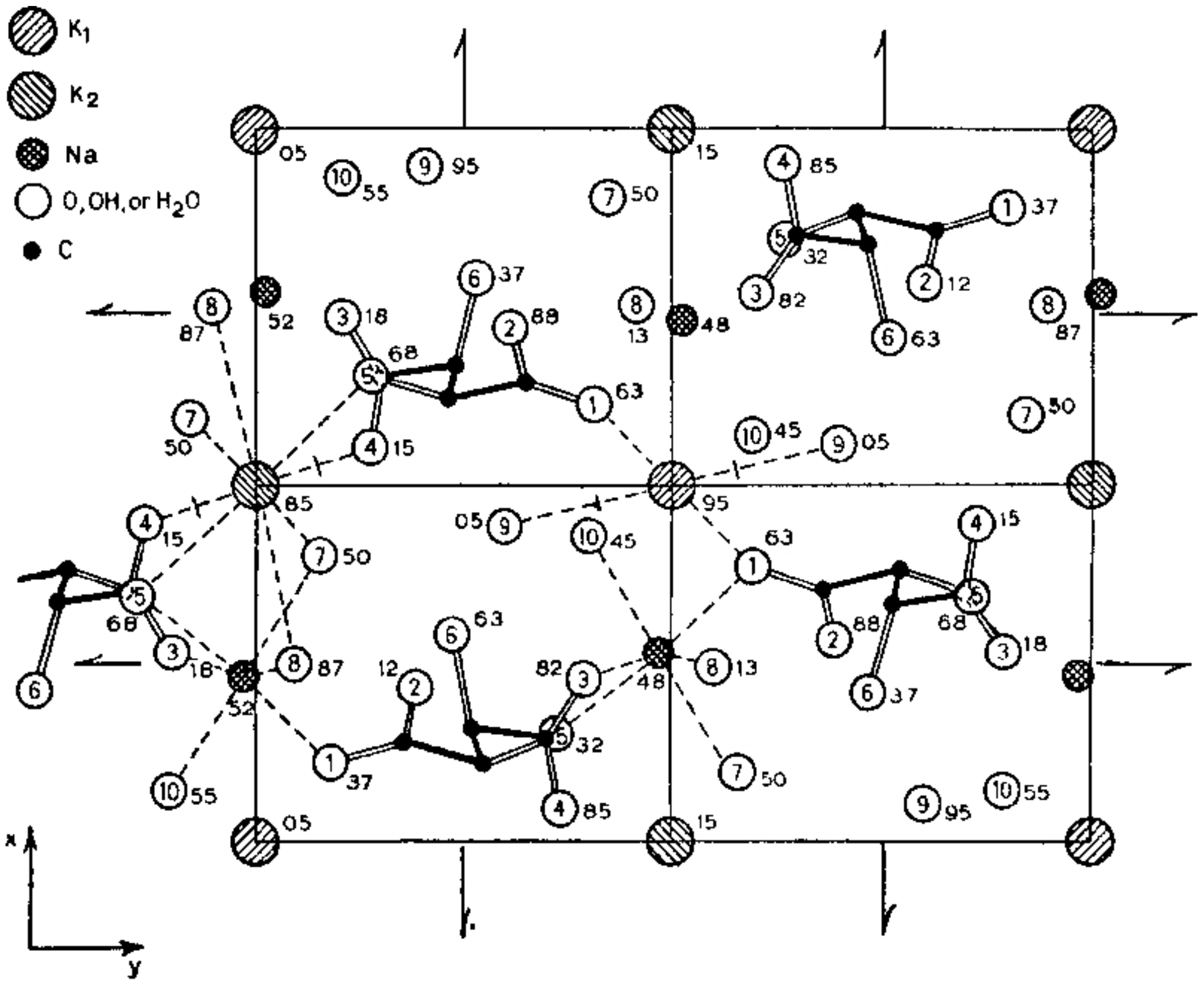

Fig. 2.1. Rochelle salt: projection of structure on 001. Figures beside atom give heights above plane $z = 0$ in hundredths of cell edge; to convert into Ångstrom units multiply by $c/100$. Positions of screw axes indicated by arrows. Environments of representative atoms shown by dotted lines; where these are crossed by a short line at right angles, they involve an atom in the cell vertically above or below that whose height is marked.

Hydrogen-bonded ferroelectricity in Rochelle's salt.

From H. W. Megaw, Ferroelectricity in Crystals, Methuen, London, 1957

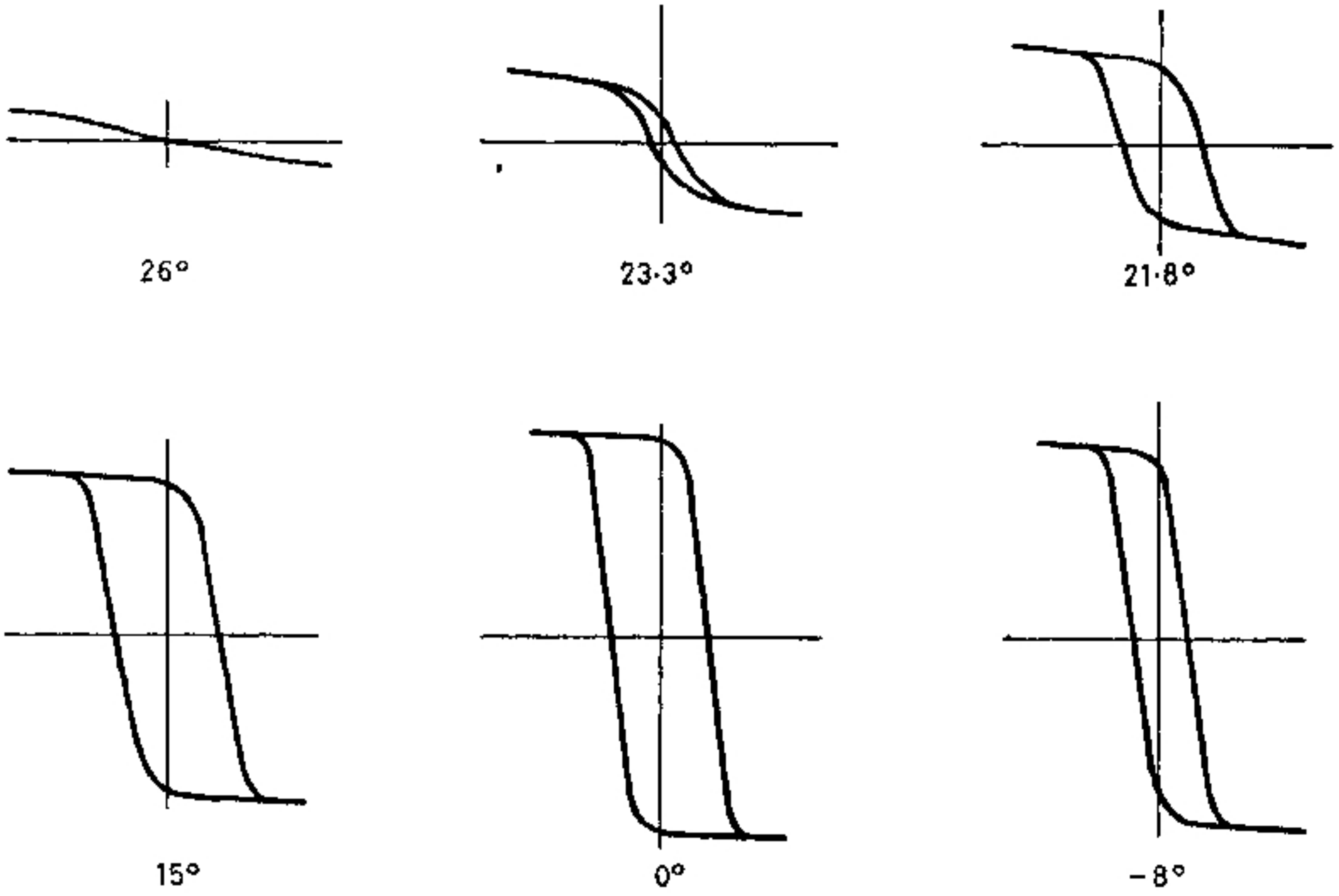

Fig. 1.5. Dielectric hysteresis loops for Rochelle salt at different tempera-
tures (Sawyer and Tower, 1930).

From H. W. Megaw, Ferroelectricity in Crystals, Methuen, London, 1957

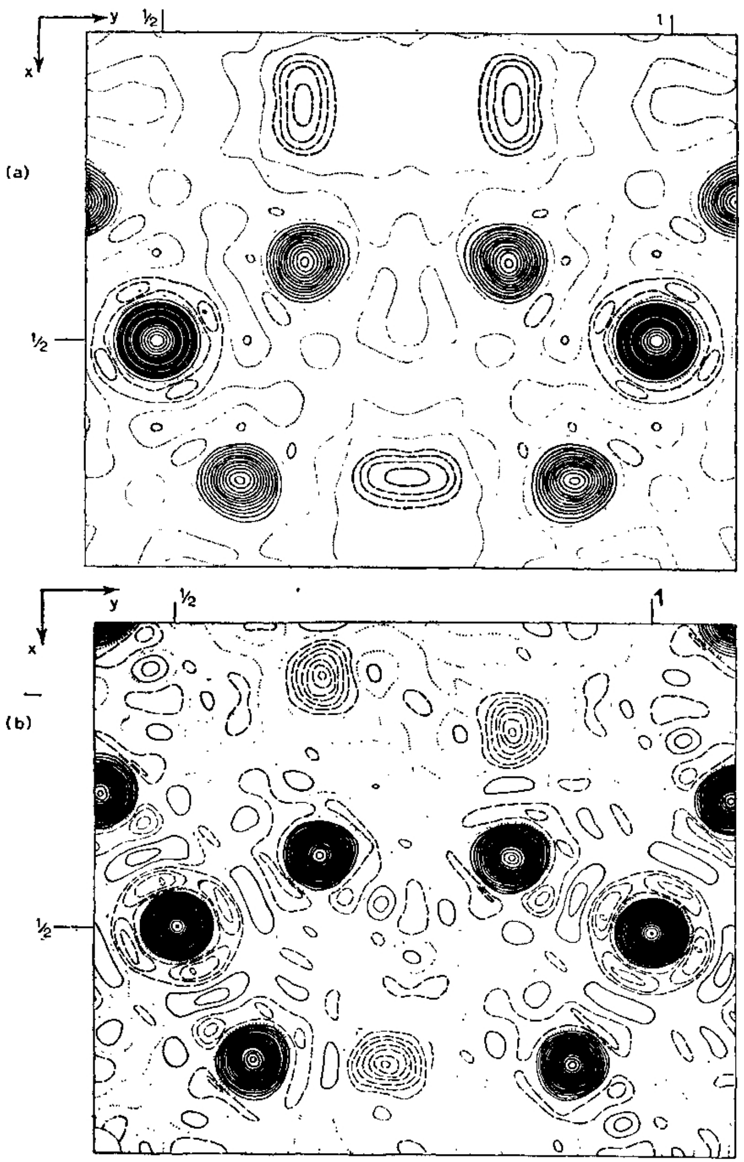

Fig. 3.3. Fourier synthesis, (001) projection, from neutron diffraction (Bacon and Pease, 1953, 1955). (*a*) at room temperature, (*b*) at 77°K.

The heaviest peaks are K + P, with O only slightly weaker; the peaks indicated by dashed contours are H. For comparison with Fig. 3.1, put the K + P peaks at $x = \frac{1}{2}, y = \frac{1}{2}$ and $x = \frac{1}{2}, y = 1$.

Hydrogen-bonded ferroelectricity in potassium dihydrogen phosphate (KDP); early neutron diffraction work.

From H. W. Megaw, Ferroelectricity in Crystals, Methuen, London, 1957

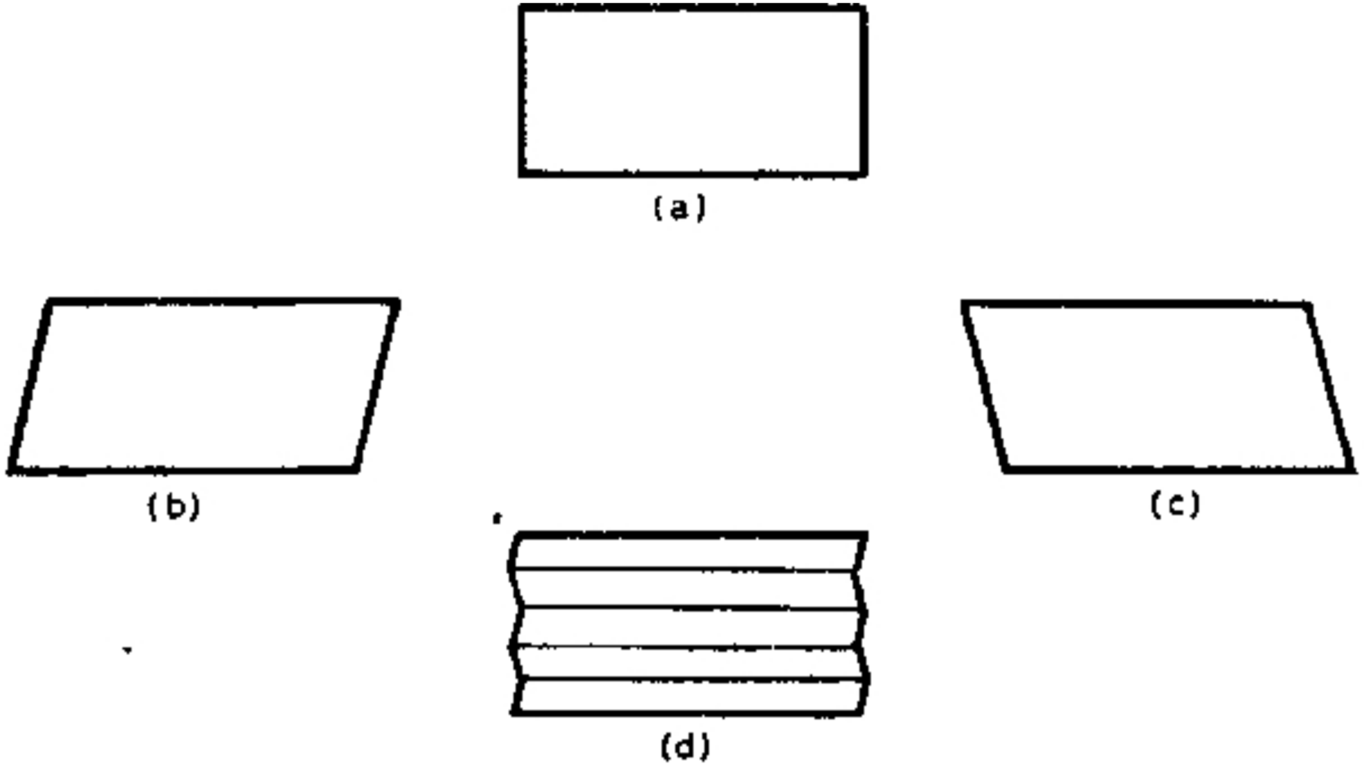

Fig. 1.6. Diagrammatic illustration of twinning in a pseudosymmetric structure.

(*a*) Crystal above transition point (high-symmetry form)
(*b*), (*c*) Low-symmetry form: two possible orientations
(*d*) Twinned crystal, with low-symmetry form in both orientations.

From H. W. Megaw, Ferroelectricity in Crystals, Methuen, London, 1957

Polar Materials and Ferroelectrics

Classification of substances related to perovskite

I. Substances occurring only in ideal cubic form	$SrTiO_3$, $SrZrO_3$, $SrHfO_3$, $SrSnO_3$, $SrFeO_3$, $BaZrO_3$, $BaHfO_3$, $BaSnO_3$, $BaCeO_3$, $EuTiO_3$, $LaMnO_3$
II. Substances having at least one form with a distorted small-cell structure (C = cubic, T = tetragonal, O = orthorhombic, R = rhombohedral, ? = doubtful or not fully investigated)	$BaTiO_3$ (C, T, O, R), $KNbO_3$ (C, T, O, R), $KTaO_3$ (C, ?), $RbTaO_3$ (C, T), $PbTiO_3$ (C, T)
III. Substances having distorted multiple-cell structures (*a*) cell size $\sqrt{2}a \times 2a \times \sqrt{2}a$ (*b*) cell size $\sqrt{2}a \times 4a \times \sqrt{2}a$ (*c*) cell size $\sqrt{2}a \times 2\sqrt{2}a \times 2a$ (*d*) cell size $2a \times 2a \times a$ (*e*) others	(*a*) $CaTiO_3$, ($CaZrO_3$), ($CdTiO_3$), ($CaSnO_3$) (*b*) $NaNbO_3$, ($NaTaO_3$) (*c*) $PbZrO_3$, $PbHfO_3$ (*d*) WO_3 (*e*) $PbTiO_3$ (low-temp.), WO_3 (high-temp.), $NaNbO_3$ (high temp.), $NaNbO_3$ (low-temp.), $LaCrO_3$
IV. Substances having structures based on close-packing (*a*) Ilmenite type (*b*) $LiNbO_3$ type	(*a*) $FeTiO_3$, $CdTiO_3$ (*b*) $LiNbO_3$, ($LiTaO_3$)

Substances in brackets have not been investigated in detail and classification is partly by analogy.

From H. W. Megaw, Ferroelectricity in Crystals, Methuen, London, 1957

Polar Materials and Ferroelectrics: $SrTiO_3$ (on the cusp of becoming ferroelectric)

Antiferrodistortive transition in $SrTiO_3$ in R-point of the Brillouin zone

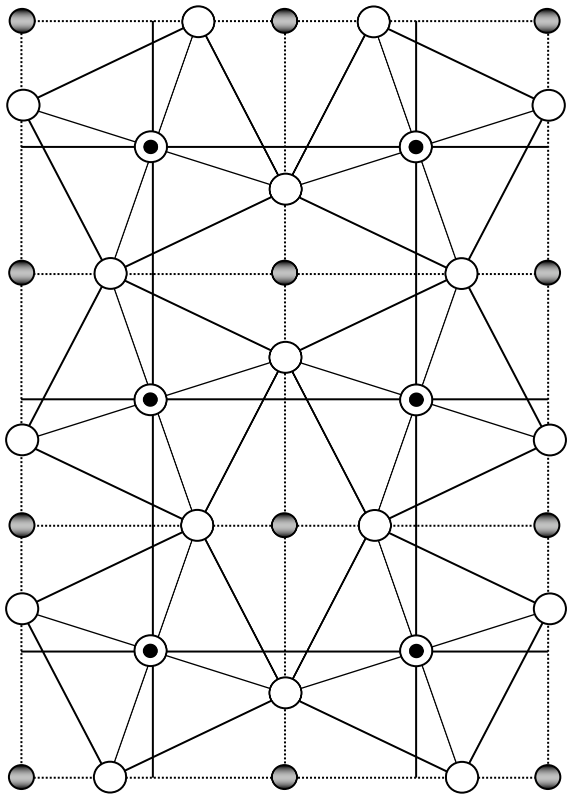

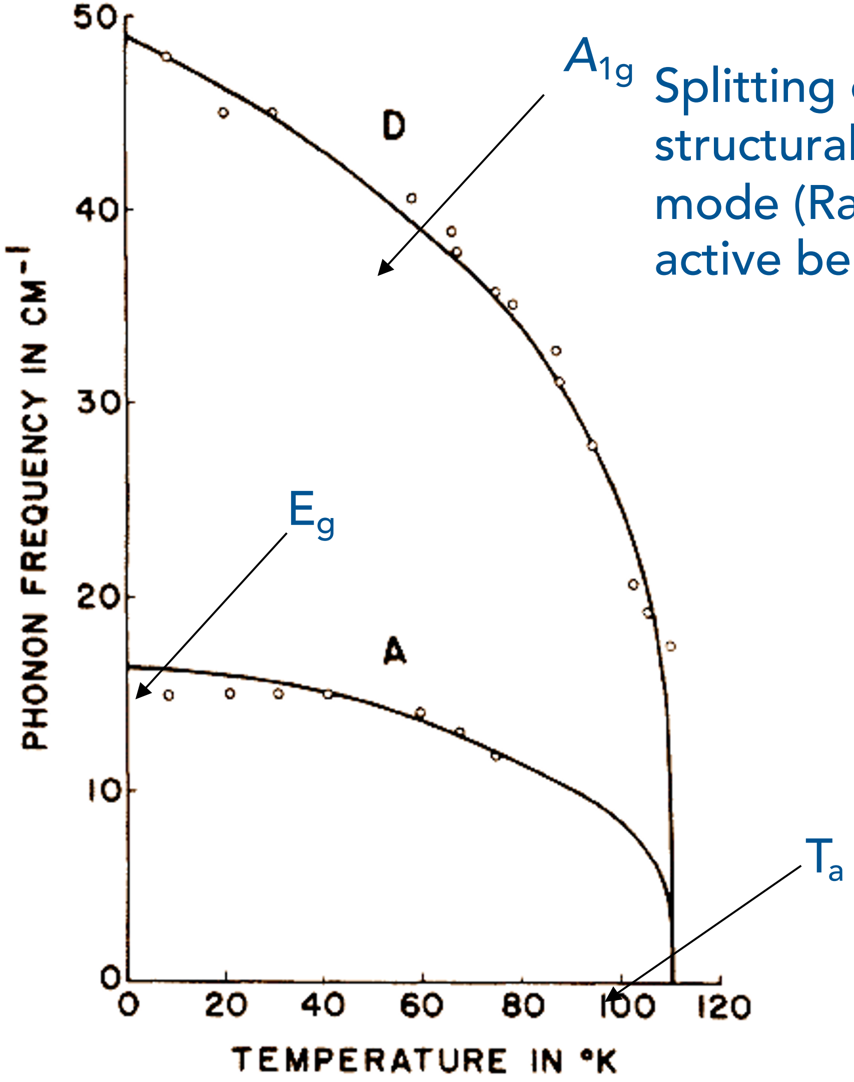

Splitting of the structural soft mode (Raman active below T_a)

Polar Materials and Ferroelectrics: $SrTiO_3$

Ferroelectric SM

Structural SM (doublet)

Mode frequencies on STO ceramics

(Petzelt *et al.*, PRB **64**, 184111 (2001))

$Pm\bar{3}m$ (O_h^1) $Z = 1$ $(P_S=0,\ T=300\ K)$			$I4/mcm$ (D_{4h}^{18}) $Z_{prim}=2$ $(P_S=0,\ T=15\ K)$		
species	activity	observed	species	activity	observed
$3F_{1u}$	IR	93,176,548	$3A_{2u}$ $3E_u$	IR	15,172,548
$1F_{2u}$	HR	266	$1B_{2u}$ $1E_u$	- IR	- -
$1R'_{15}(F_{1g})$	N	$\sim$40 (soft)	$1A_{1g}$ $1E_g$	R	52 40
$2R'_{25}(F_{2g})$	-	-	$2B_{1g}$ $2E_g$	R	144,447
$1R_{15}(F_{1u})$	-	-	$1A_{1u}$ $1E_u$	- IR	- 436
$1R_{12}(E_g)$	-	-	$1A_{2g}$ $1B_{2g}$	- R	- 229
$1R_1(A_{1g})$	-	-	$1A_{2g}$	-	-
Total (Γ point)	$3F_{1u}+1F_{2u}$		$1A_{1g}+1A_{1u}+2A_{2g}+3A_{2u}+$ $+2B_{1g}+2B_{2g}+2B_{2u}+3E_g+3E_u$		
Mode activity	3 IR		$8\mathrm{IR}+7R$		

Polar Materials and Ferroelectrics: $SrTiO_3$

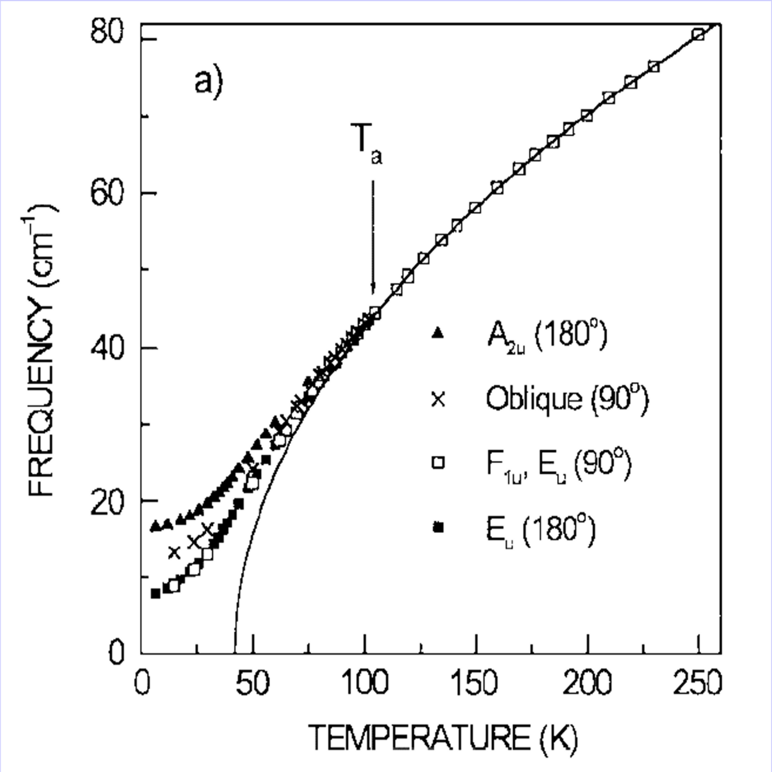

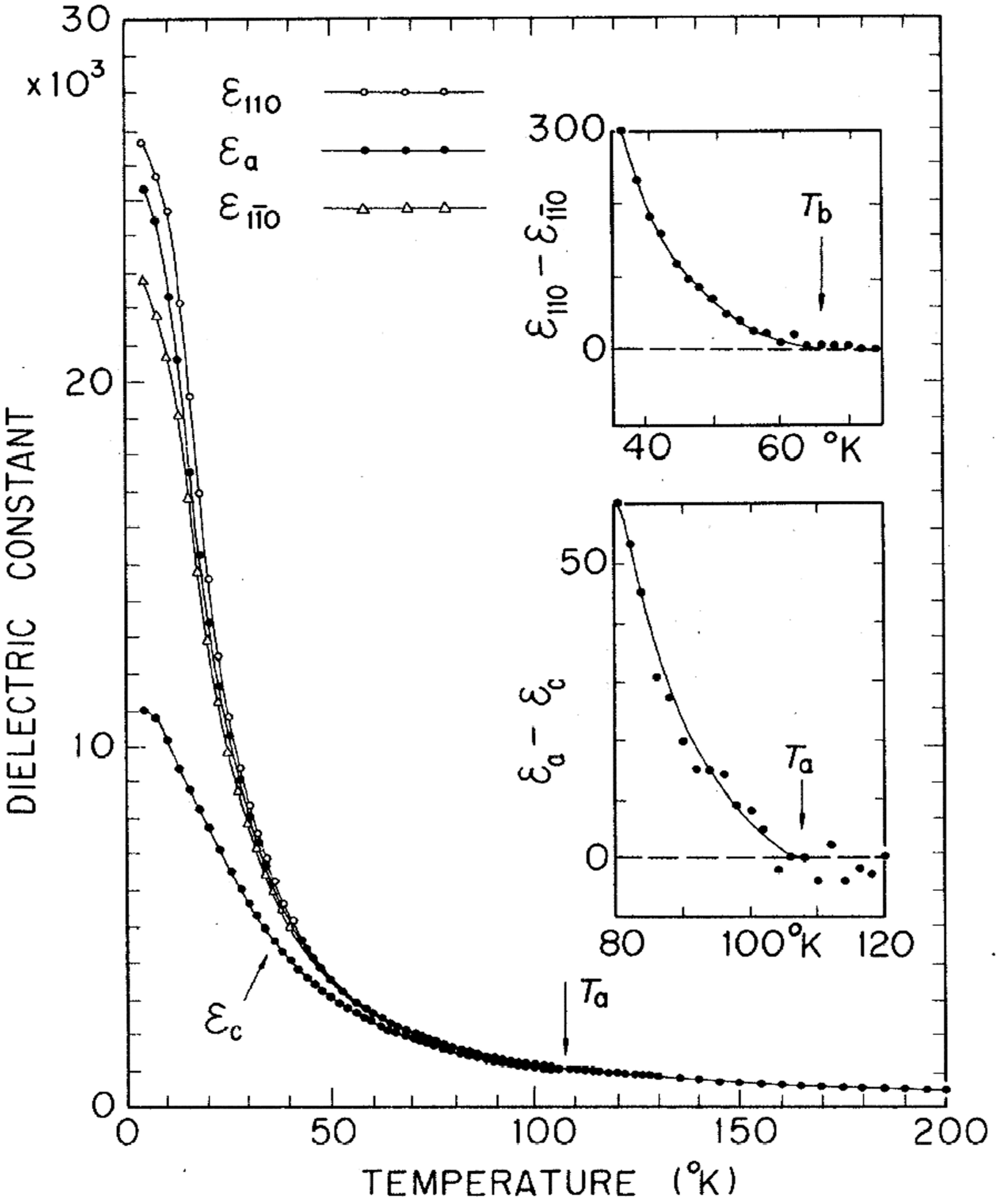

SANTA BARBARA

Polar Materials and Ferroelectrics: $SrTiO_3$

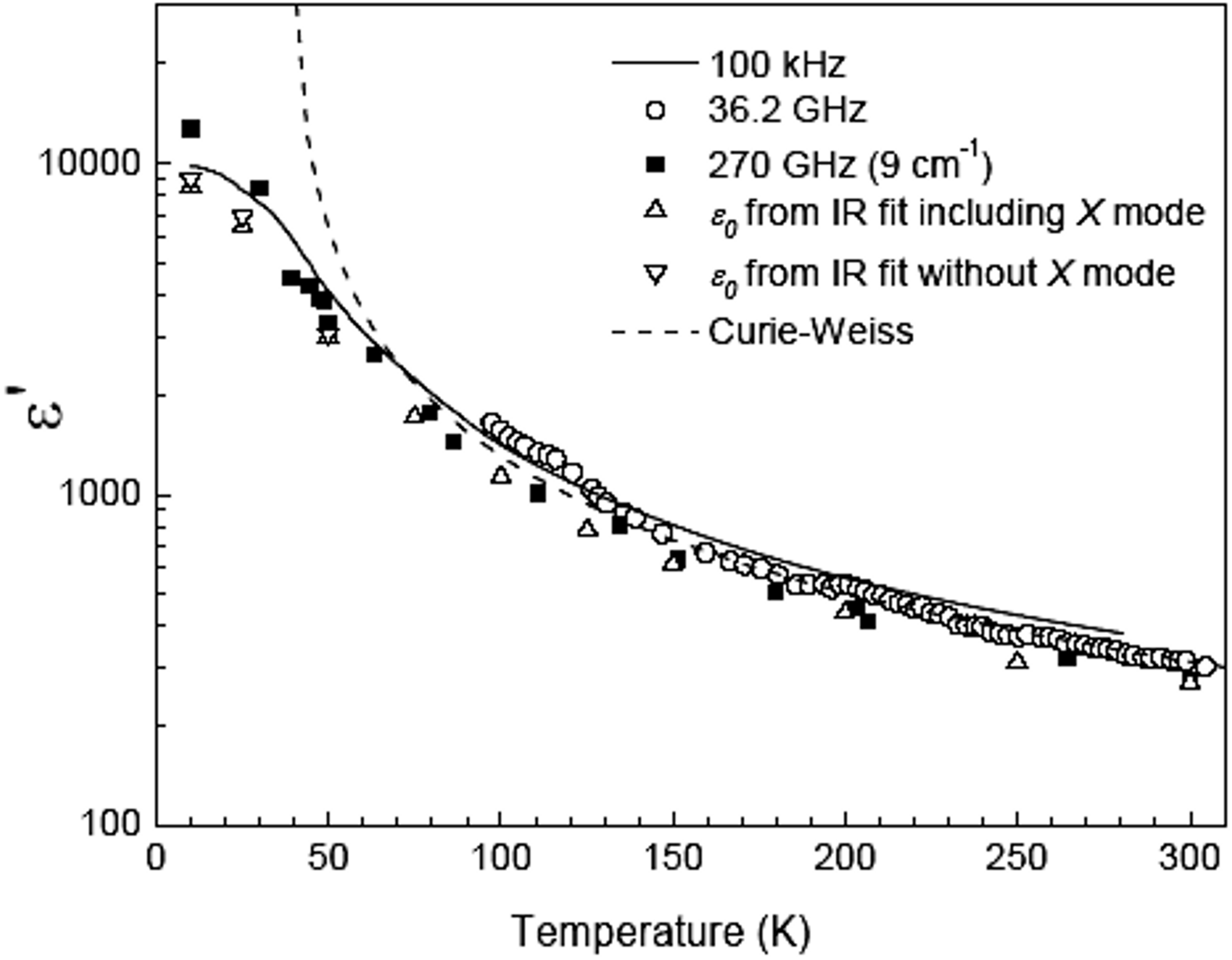

UC SANTA BARBARA

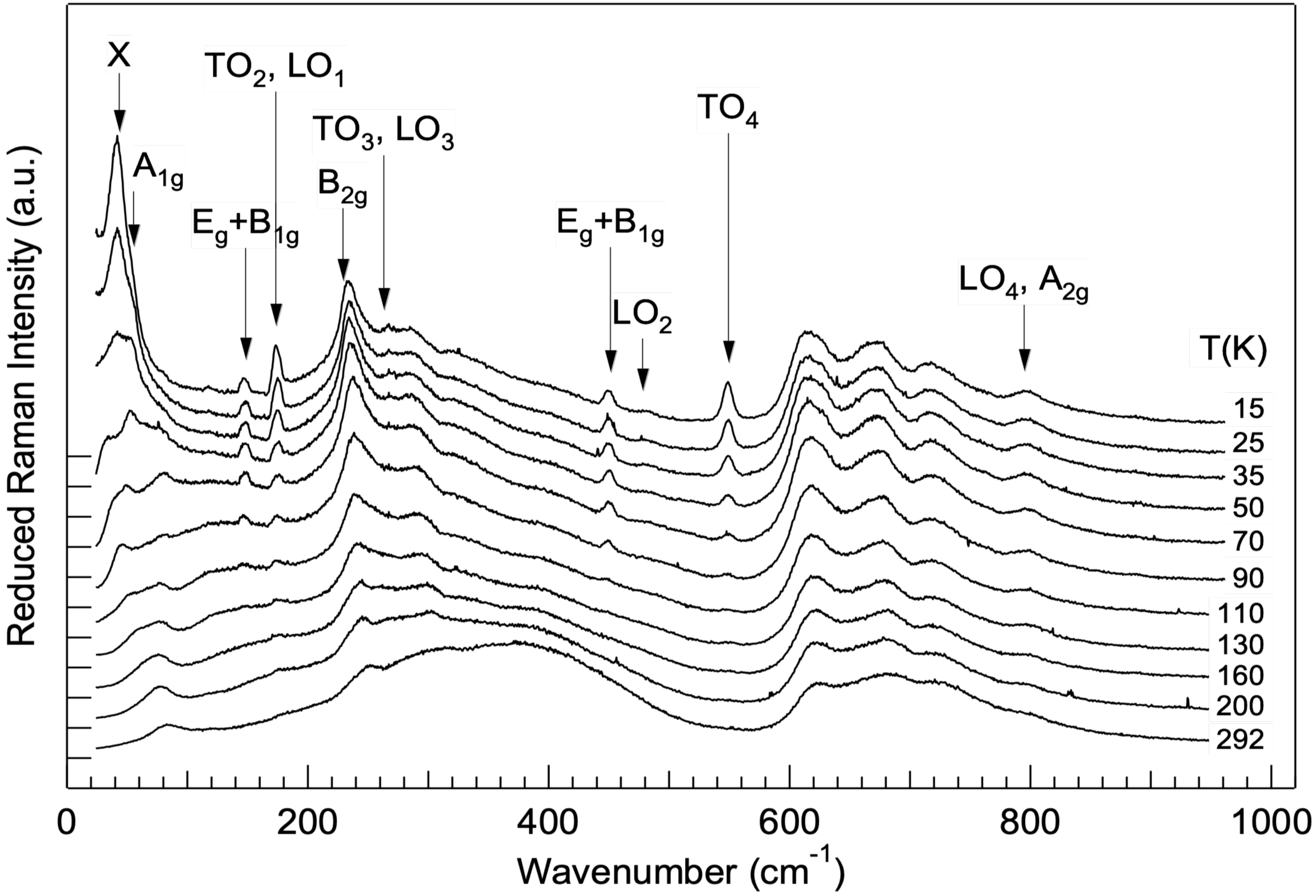
X
TO2, LO1
TO3, LO3
A1g
B2g
Eg+B1g
Eg+B1g
LO2
TO4
LO4, A2g
T(K)
15
25
35
50
70
90
110
130
160
200
292
Reduced Raman Intensity (a.u.)
0
200
400
600
800
1000
Wavenumber (cm-1)

Polar Materials and Ferroelectrics: $SrTiO_3$

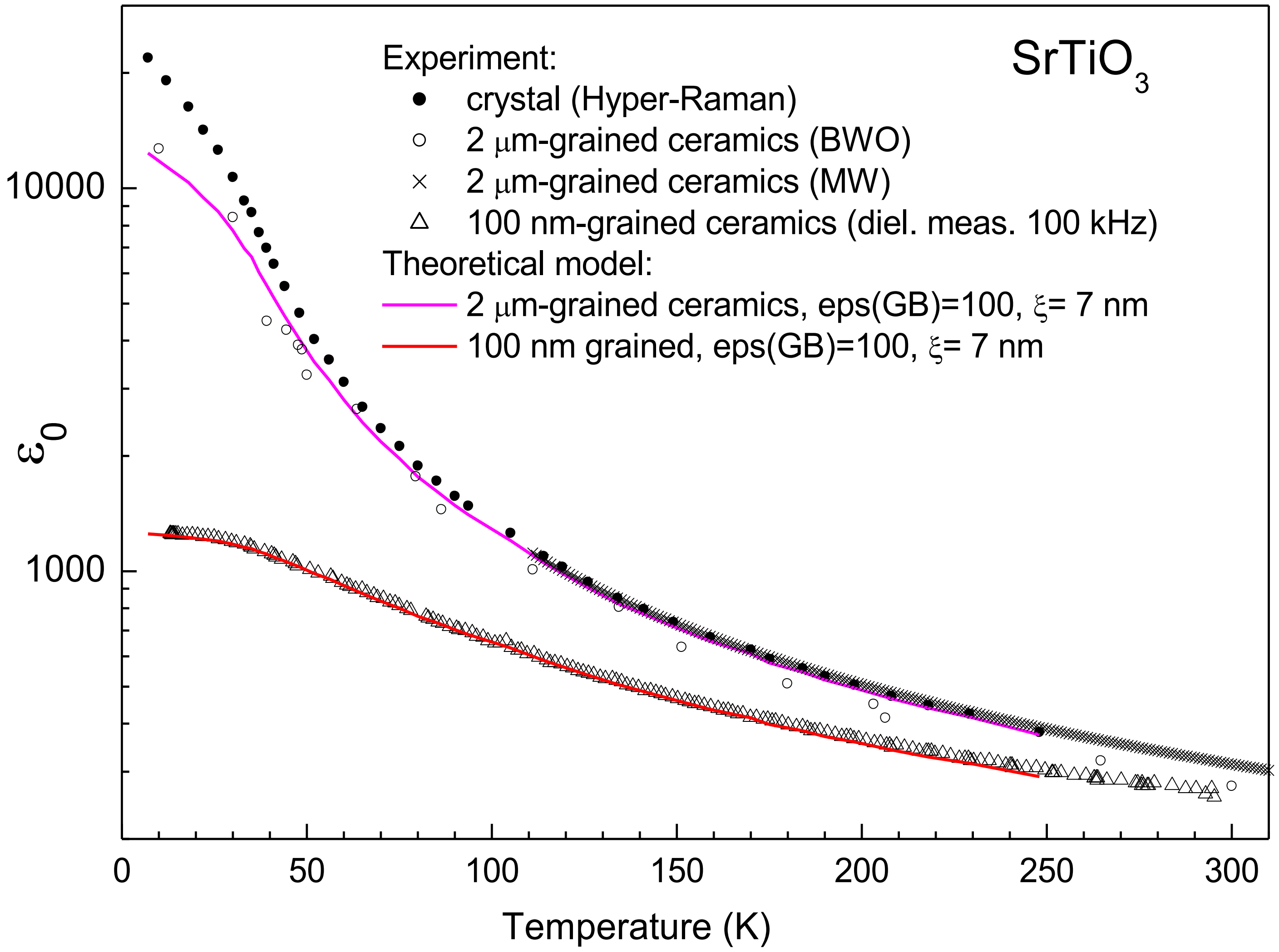

Order-disorder model for $BaTiO_3$ phase transitions

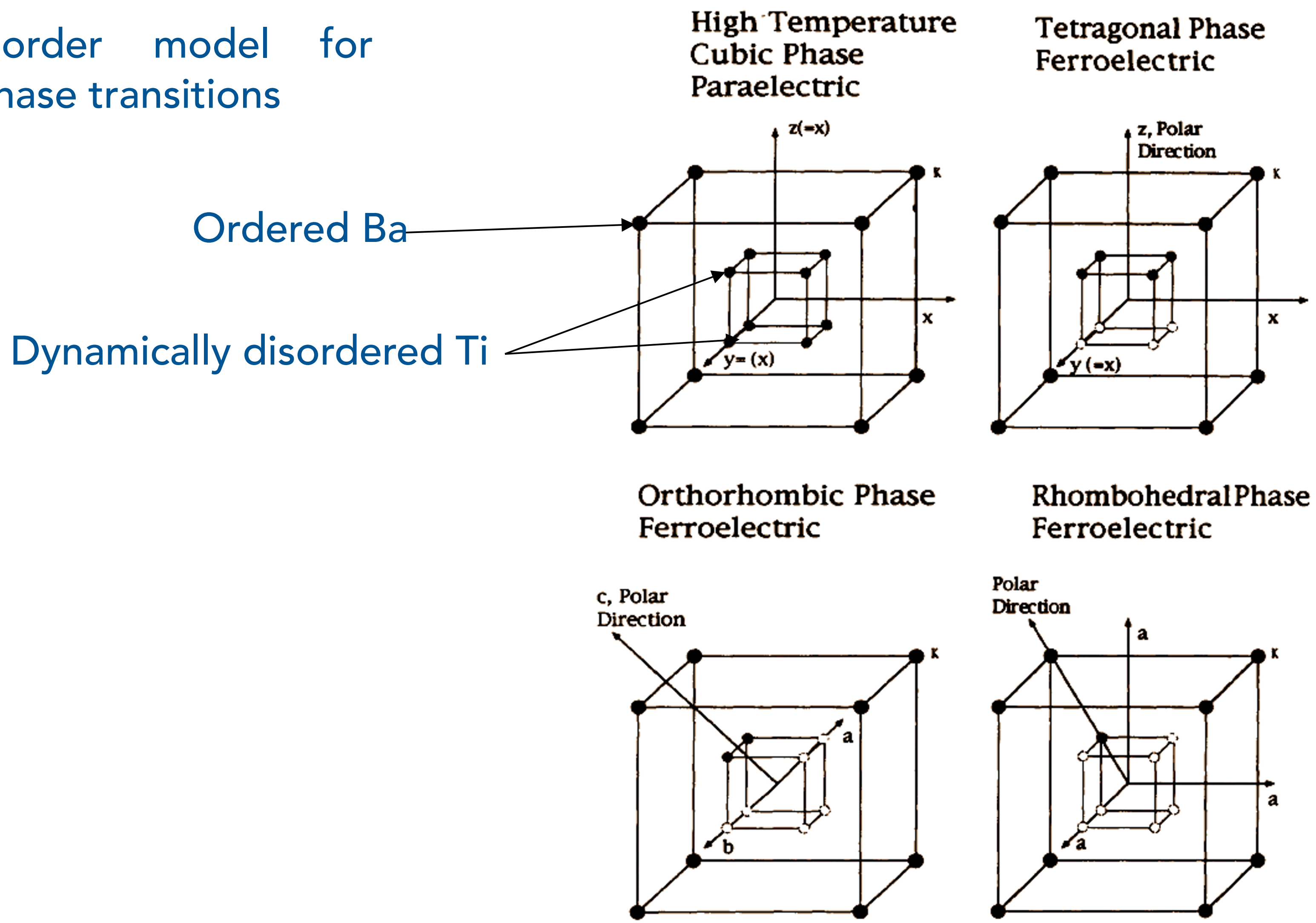

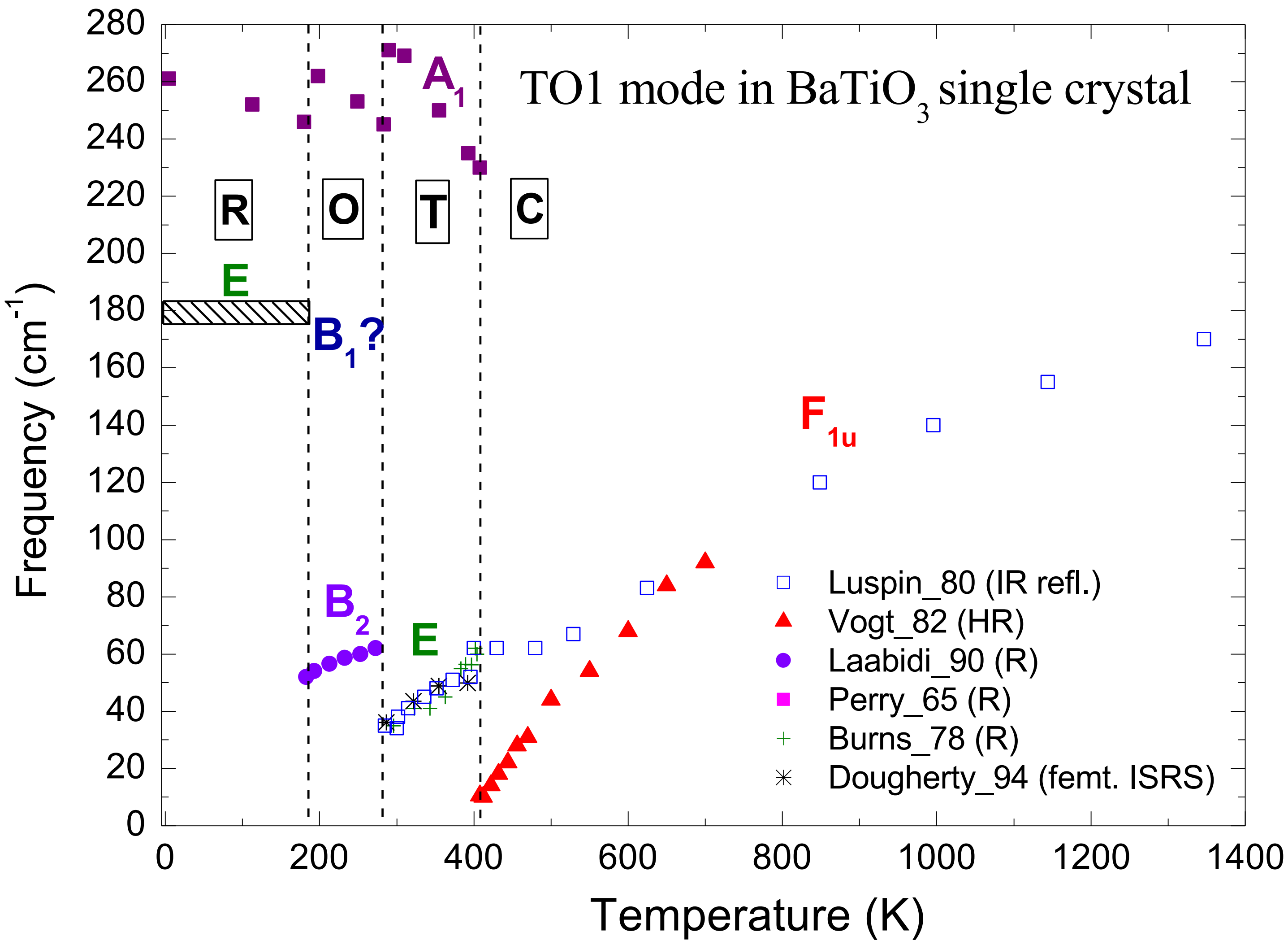
TO1 mode in $BaTiO_3$ single crystal
R
O
T
C
A_1
E
B_1?
B_2
E
F_{1u}
Luspin_80 (IR refl.)
Vogt_82 (HR)
Laabidi_90 (R)
Perry_65 (R)
Burns_78 (R)
Dougherty_94 (femt. ISRS)
Frequency (cm^{-1})
Temperature (K)
0
20
40
60
80
100
120
140
160
180
200
220
240
260
280
0
200
400
600
800
1000
1200
1400

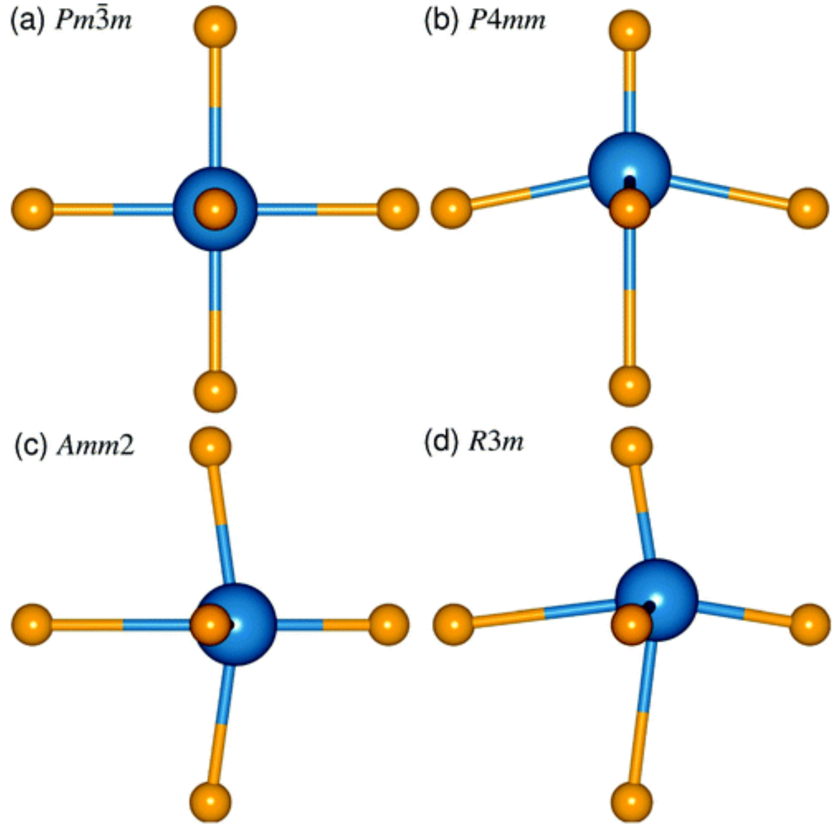
(a) $Pm\bar{3}m$
(b) $P4mm$
(c) $Amm2$
(d) $R3m$

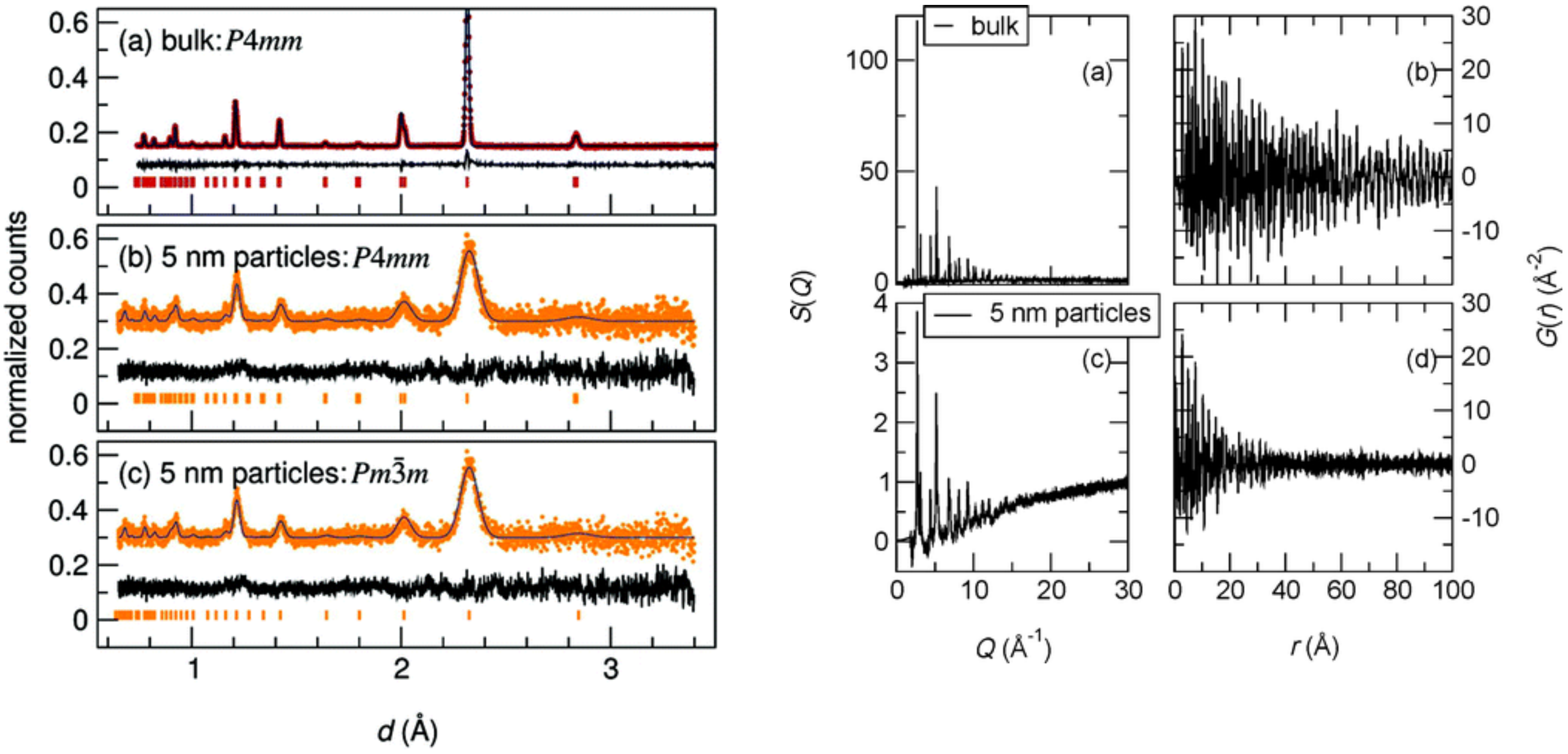

(a) bulk: P4mm
(b) 5 nm particles: P4mm
(c) 5 nm particles: Pm$\bar{3}$m
normalized counts
d (Å)
bulk
5 nm particles
(a)
(b)
(c)
(d)
S(Q)
G(r) (Å^-2)
Q (Å^-1)
r (Å)

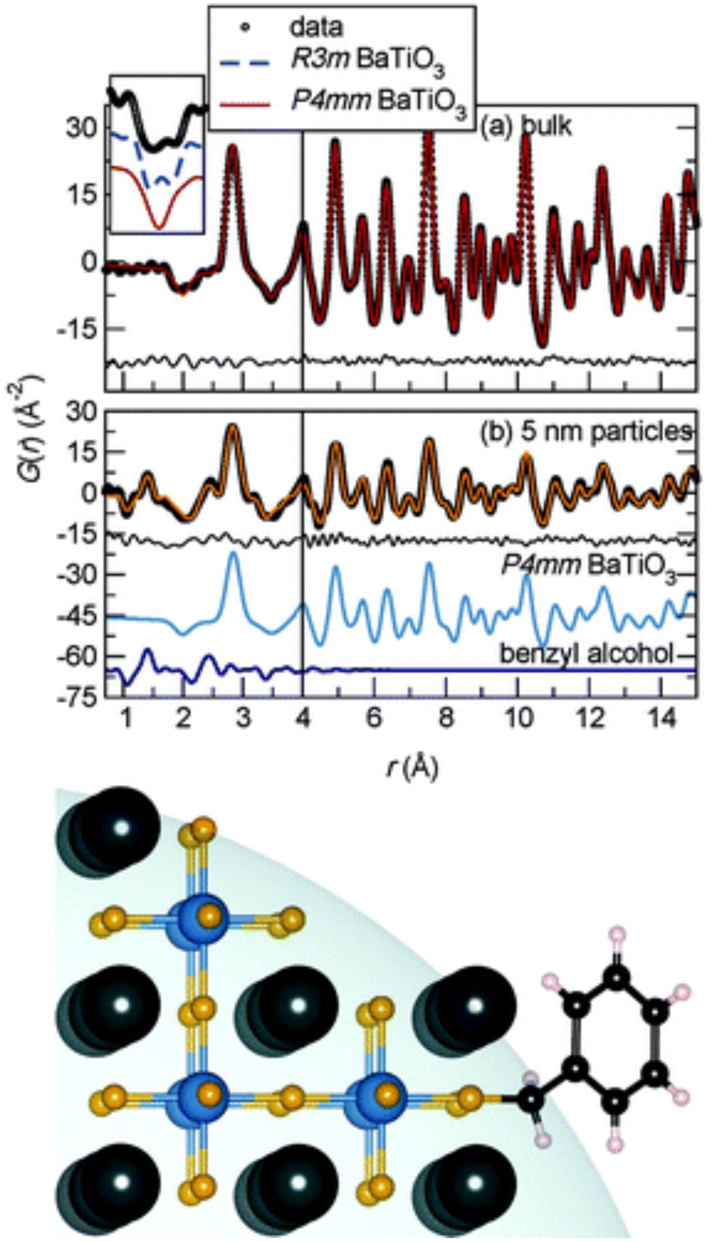

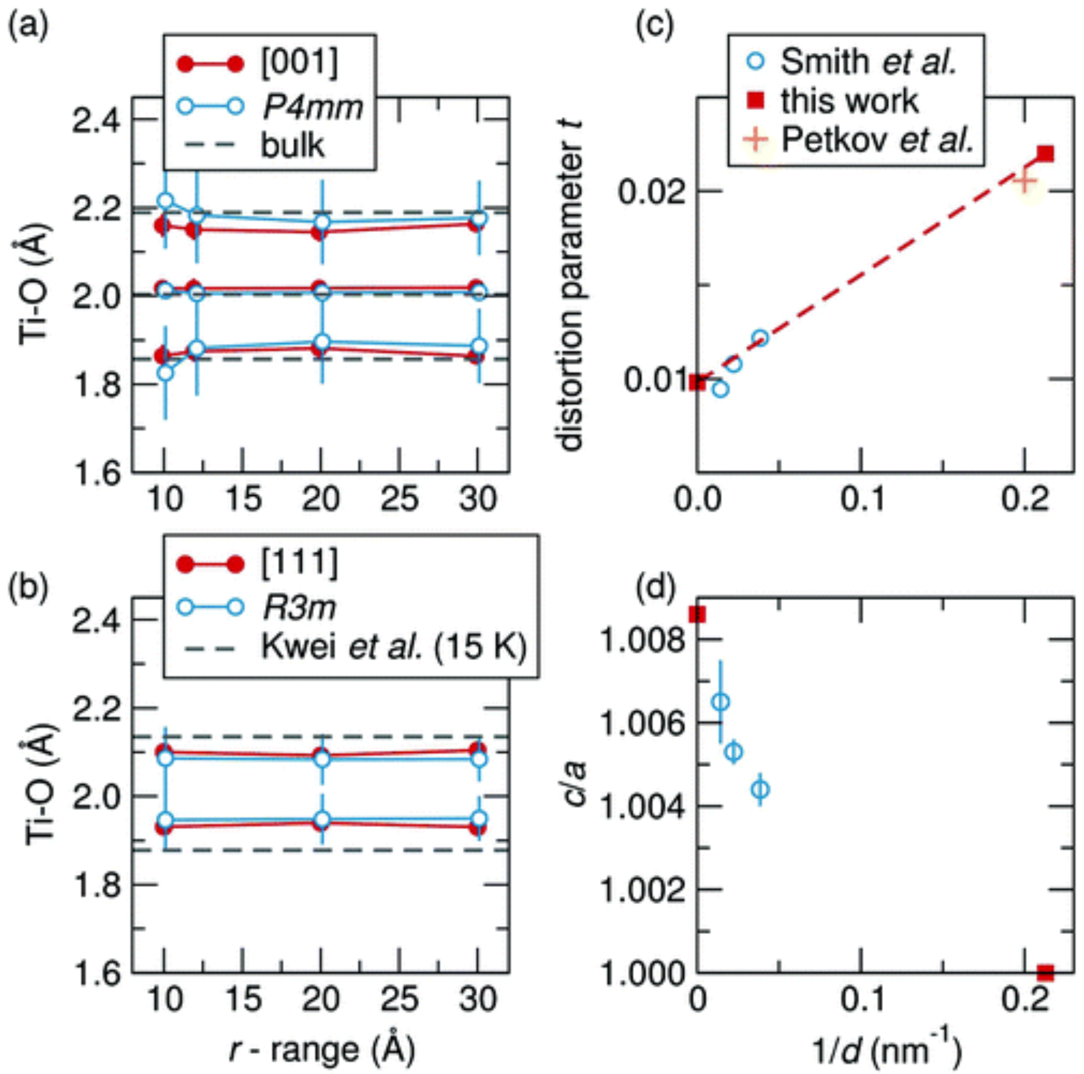

Page, Proffen, Niederberger, Seshadri, Probing local dipoles and ligand structure in $BaTiO_3$ nanoparticles, *Chem. Mater.* **22** (2010) 4386–4391.

Antiferroelectrics: The example of $PbZrO_3$